Bioorganic & Medicinal Chemistry Letters 22 (2012) 3951–3956

Contents lists available at SciVerse ScienceDirect

Bioorganic & Medicinal Chemistry Letters

journal homepage: www.elsevier.com/locate/bmcl

Pyrazole and pyrimidine phenylacylsulfonamides as dual Bcl-2/Bcl-xL antagonists

Gretchen M. Schroeder [a,*,†], Donna Wei [a,†], Patrizia Banfi [b], Zhen-Wei Cai [a,‡], Jonathan Lippy [a], Maria Menichincheri [b], Michele Modugno [b], Joseph Naglich [a], Becky Penhallow [a], Heidi L. Perez [a], John Sack [a], Robert J. Schmidt [a], Andrew Tebben [a], Chunhong Yan [a], Liping Zhang [a], Arturo Galvani [b], Louis J. Lombardo [a,§], Robert M. Borzilleri [a]

[a] Bristol-Myers Squibb Research, PO Box 4000, Princeton, NJ 08543-4000, USA
[b] Nerviano Medical Sciences Srl, Oncology, Viale Pasteur 10, 20014 Nerviano (MI), Italy

ARTICLE INFO

Article history:
Available online 30 April 2012

Keywords:
Bcl-2
Bcl-xL
Isolated mitochondria
Protein–protein interaction
Cytochrome c

ABSTRACT

5-Butyl-1,4-diphenyl pyrazole and 2-amino-5-chloro pyrimidine acylsulfonamides were developed as potent dual antagonists of Bcl-2 and Bcl-xL. Compounds were optimized for binding to the I88, L92, I95, and F99 pockets normally occupied by pro-apoptotic protein Bim. An X-ray crystal structure confirmed the proposed binding mode. Observation of cytochrome c release from isolated mitochondria in MV-411 cells provides further evidence of target inhibition. Compounds demonstrated submicromolar antiproliferative activity in Bcl-2/Bcl-xL dependent cell lines.

The B-cell lymphoma 2 (Bcl-2) family of proteins are key mediators of apoptosis or programmed cell death.[1] Anti-apoptotic family members including Bcl-2, Bcl-xL, and Mcl-1 bind and sequester pro-apoptotic members such as Bim, Puma, Noxa, Bad, and Bax, thereby preventing mitochondria-mediated cell death. Dysregulation of this critical process has been implicated in cancer. For example, up-regulation of anti-apoptotic family members provides a mechanism for cells to evade apoptosis, allowing for tumorigenesis and resistance to chemotherapy and radiation.

Protein–protein interactions have proven challenging targets in drug discovery as they are frequently characterized as large, diffuse, and solvent-exposed.[2] Despite these challenges, small molecule protein mimetics have made considerable progress in recent years. In particular, α-helix mimetics have been described by a number of groups to disrupt protein–protein interactions.[3] Bcl-2 family proteins interact through binding of α-helical pro-apoptotic Bcl-2 family members to a conserved hydrophobic groove present on anti-apoptotic family members. Small molecule inhibitors of this heterodimerization event have been described for anti-apoptotic proteins Bcl-2 and Bcl-xL.[4,5] The most advanced Bcl-2 inhibitor currently in human clinical trials, ABT-263 (**1**), demonstrates single agent activity in xenograft models of small-cell lung cancer and acute lymphoblastic leukemia as well as the ability to potentiate the effects of cytotoxic agents in B-cell lymphoma and multiple myeloma where single agent activity is modest or absent (Fig. 1).[6,7] While ABT-263 (**1**) has generated considerable interest, albumin binding has been shown to greatly diminish sensitivity of chronic lymphocytic leukemia (CLL) cells to ABT-263 (**1**) and may limit the effectiveness of this promising agent in vivo.[8]

In the preceding paper, we described a novel series of pyrazole-derived phenylacylsulfonamides **2** as potent dual Bcl-2/Bcl-xL antagonists (Fig. 1).[9] We have further developed this initial lead series to generate additional potent dual Bcl-2/Bcl-xL antagonists from two distinct chemotypes with improved cellular activity. Herein we describe the synthesis and SAR of regiosiomeric pyrazoles **3** and 2-aminopyrimidines **4**.

A versatile synthetic route to the target regioisomeric pyrazoles was developed to allow for substitution of the pyrazole, tetrahydroisoquinoline (THIQ), and acyl sulfonamide moieties (Scheme 1). Commercially available 3-(*tert*-butoxycarbonyl)benzoic acid (**5**) was first selectively iodinated in the ortho position to give 2-iodo acid **6**.[10] Following amide formation with THIQ **7**, the iodide was then carbonylated to give aldehyde **9**. Use of trioctylsilane in this reaction was critical as the more typical (and more reactive) triethylsilane prematurely reduced the aryl-halide bond before CO insertion could occur. Aldehyde **9** was then converted to nitroalcohol **10**

* Corresponding author. Tel.: +1 609 252 3965.
E-mail address: gretchen.schroeder@bms.com (G.M. Schroeder).
† Authors contributed equally to the composition of this manuscript.
‡ Current address: PharmaResources (Shanghai) Co., Ltd, Building 1B, No. 528 RuiQing Rd., Pudong, Shanghai 201201, PR China.
§ Current address: Hoffman-La Roche Inc., 340 Kingsland Street, Nutley, NJ 07110, USA.

0960-894X/$ - see front matter © 2012 Elsevier Ltd. All rights reserved.
http://dx.doi.org/10.1016/j.bmcl.2012.04.106

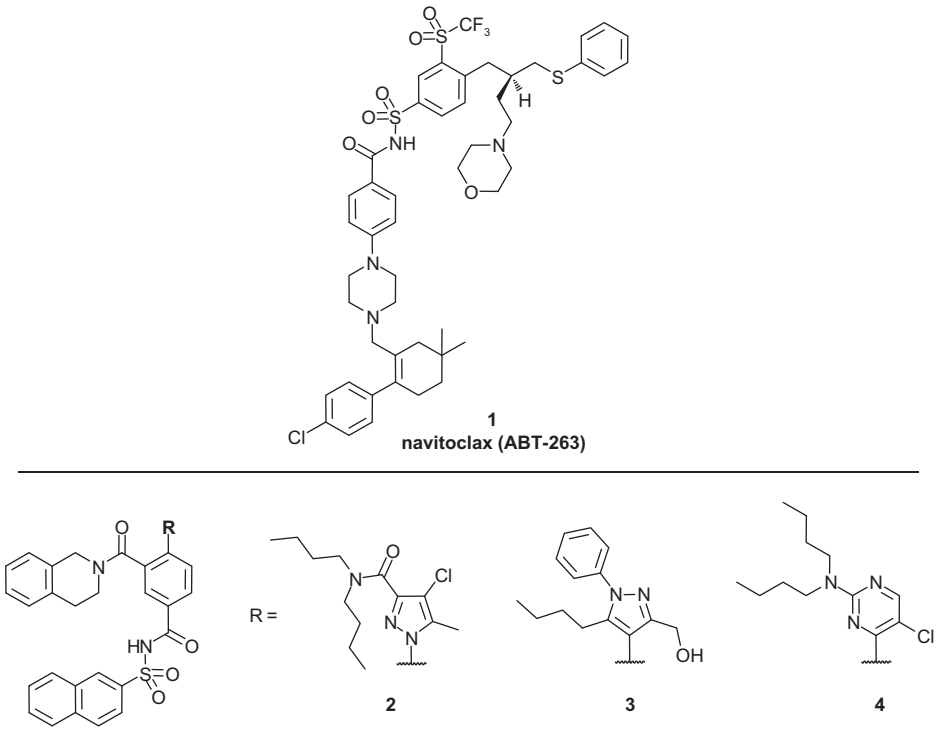

Figure 1. Bcl-2 family antagonists.

which was itself dehydrated to give nitroolefin **11** in good yield over two steps. The pyrazole ring was then constructed with complete regiocontrol by reaction of the appropriately substituted hydrazone **12** in the presence of potassium *tert*-butoxide followed by a TFA quench.[11] Finally, deprotection of the *tert*-butyl ester followed by acylsulfonamide formation gave the desired compounds **3**.

The ethyl ester present in pyrazole **3b** could be further derivatized to give the corresponding acid **3c** by hydrolysis with aqueous sodium hydroxide. Careful reduction of the ethyl ester with lithium borohydride could also be achieved to give the alcohol **3d**.

Preparation of 2-aminopyrimidine phenylacylsulfonamides **4** is shown in Scheme 2. Aryl boronate **16** was prepared according to the method reported by Miura and coworkers.[12] Suzuki coupling of boronate **16** with 2,4-dichloropyrimidine (R^2 = H), 2,4-dichloro-5-methylpyrimidine (R^2 = methyl), or 2,4,5-trichloropyrimidine (R^2 = Cl) chemoselectively afforded the corresponding biaryl **17**. Displacement of the 2-chloride on the pyrimidine ring with different dialkylamines provided 2-aminopyrimidine intermediate **18**. After removing the Boc protecting group, tetrahydroisoquinolines were introduced by HATU-mediated coupling. Hydrolysis of methyl ester **19** under basic conditions afforded the corresponding acids which were coupled with sulfonamides **15** to form analogs **4a**–**e**. The synthetic sequence was flexible in that the order of steps for the acylsulfonamide and THIQ amide formation could be reversed to give **4f**–**g**, allowing for more efficient survey of THIQ substituents or replacements. Finally, (*S*) 3-aminomethyl THIQ **4h** was prepared from the corresponding azide by palladium catalyzed hydrogenation.

We began by exploring SAR of the regioisomeric pyrazoles **3** with initial efforts directed at exploring the pyrazole ring itself (Table 1). The alkyl group at C-5 was examined and it was determined that small alkyl groups gave inferior results as compared to larger alkyl groups. For example, methyl substituted pyrazole **3a** was only 4.19 and 0.64 μM versus Bcl-2 and Bcl-xL, respectively whereas, butyl substituted pyrazole **3b** showed nearly 10-fold improvement against both proteins (0.66 μM versus Bcl-2 and 0.042 μM versus Bcl-xL). Alteration of the ethyl ester at the pyrazole C-3 position also significantly impacted Bcl-2 and Bcl-xL activity. For example, acid **3c** saw further improvements in both Bcl-2 and Bcl-xL activity (0.17 μM and 0.030 μM, respectively). Alcohol **3d** was optimum giving an IC_{50} of 61 nM for Bcl-2 and 11 nM for Bcl-xL. Substitution of the pyrazole *N*-1 aryl group was studied extensively. Small alkoxy substituents in the para position of the pyrazole *N*-phenyl ring were generally tolerated (i.e., methoxy compound **3e**). Addition of a larger, more lipophilic phenoxy group in the meta (**3f**) and para (**3g**) positions was examined. While both analogs gave enhanced activity versus Bcl-2, only the para substitution was tolerated for Bcl-xL.

Encouraged by the improved dual inhibition demonstrated by phenyl ether **3g**, we examined this lead further. As observed before, reduction of the ethyl ester to give alcohol **3h** was well tolerated. Addition of a chloride to the phenoxy ring gave an additional increase in activity. The 3-chlorophenyl derivative **3j** was superior to the 4-chlorophenyl analog **3i** inhibiting Bcl-2 with an IC_{50} of 8 nM and Bcl-xL with an IC_{50} of 18 nM. Replacement of the phenoxy group with butoxy (**3k**) gave a modest reduction in Bcl-2 and Bcl-xL activity. Elimination of the ether linker to give biphenyl **3l** was well tolerated and inhibited Bcl-2 and Bcl-xL with IC_{50}'s of 7 and 13 nM, respectively. Recognizing that inhibitors of protein–protein interactions tend to be rather lipophilic with high clogP's, we examined appending alcohols to the pyrazole *N*-phenyl ring to improve aqueous solubility and create more drug-like leads. To that end, para alcohols **3m** and **3n** were generated and, gratifyingly, the appended alcohols were also well accommodated by both Bcl-2 and Bcl-xL. A meta substituted alcohol **3o** was slightly less active than its para counterparts.

Next we turned our attention to SAR of the tetrahydroisoquinoline ring (Table 2). Borrowing from our previous experience with substituted THIQs,[9] we prepared alcohol **3p**. As expected, this compound demonstrated a marked improvement in Bcl-2 potency relative to the unsubstituted THIQ **3d**, generating a potent dual

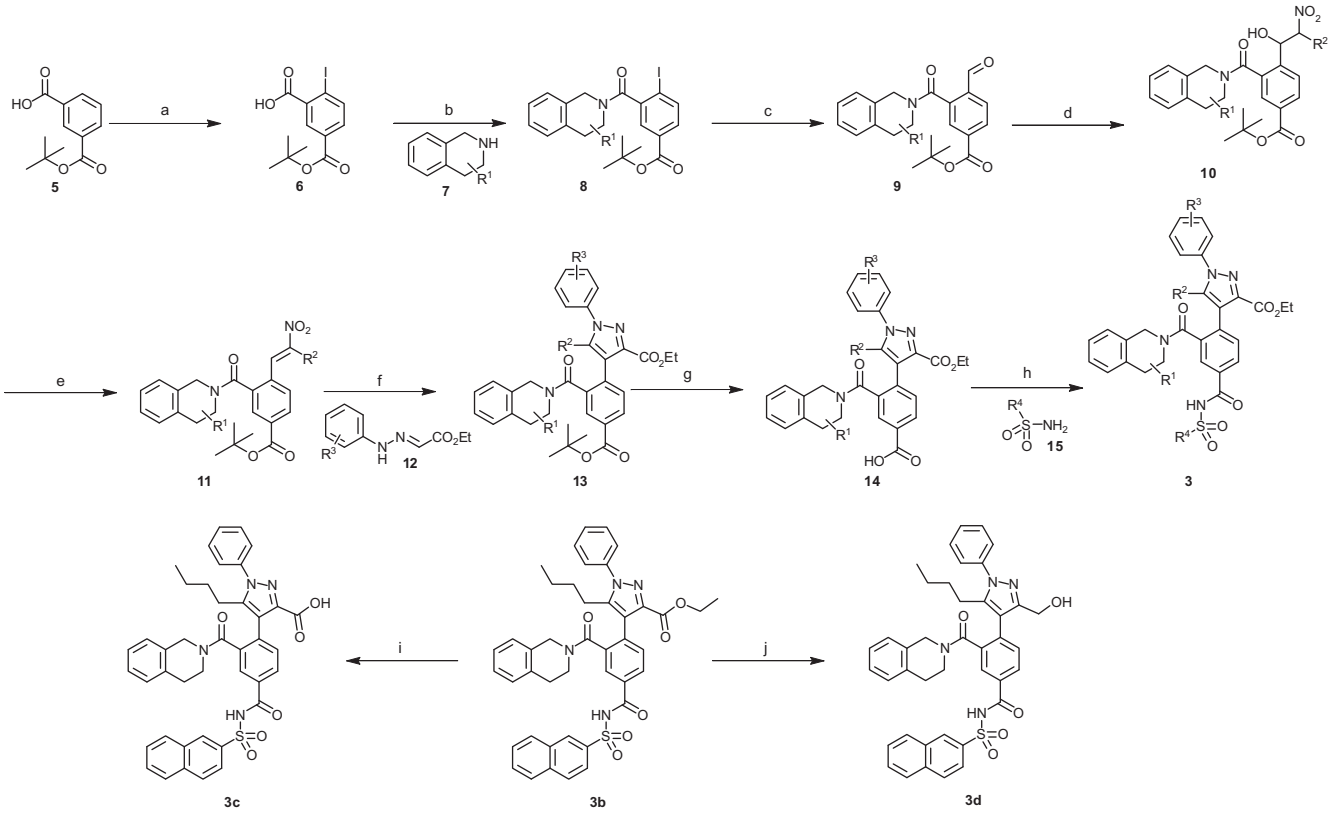

Scheme 1. Reagents and conditions: (a) $Pd(OAc)_2$, $PhI(OAc)_2$, I_2, Bu_4NI, DCE, 80 °C, 6 h, 62%; (b) HATU, 2,6-lutidine, THF/DMF, rt, 1 h, 54–65%; (c) $Pd(dppf)Cl_2$, Oct_3SiH, DIPEA, CO, DMF, 70 °C, 16 h, 40–50%; (d) $R^2CH_2NO_2$, KO*t*Bu, THF, rt, 3 h; (e) Ac_2O, cat. DMAP, THF, rt, 30 min, then DMAP, DCM, rt, 16 h, 66–80% (2 steps); (f) KO*t*Bu, THF, −78 °C, then TFA, −78 °C, 2 h, 17–68%; (g) TFA, DCM, rt, 1 h; (h) EDC, DMAP, DMF, rt, 24–90% (2 steps); (i) 1 N aqueous NaOH, THF, rt, 16 h, 100%; (j) $LiBH_4$, THF, rt, 2 h, 64–55%.

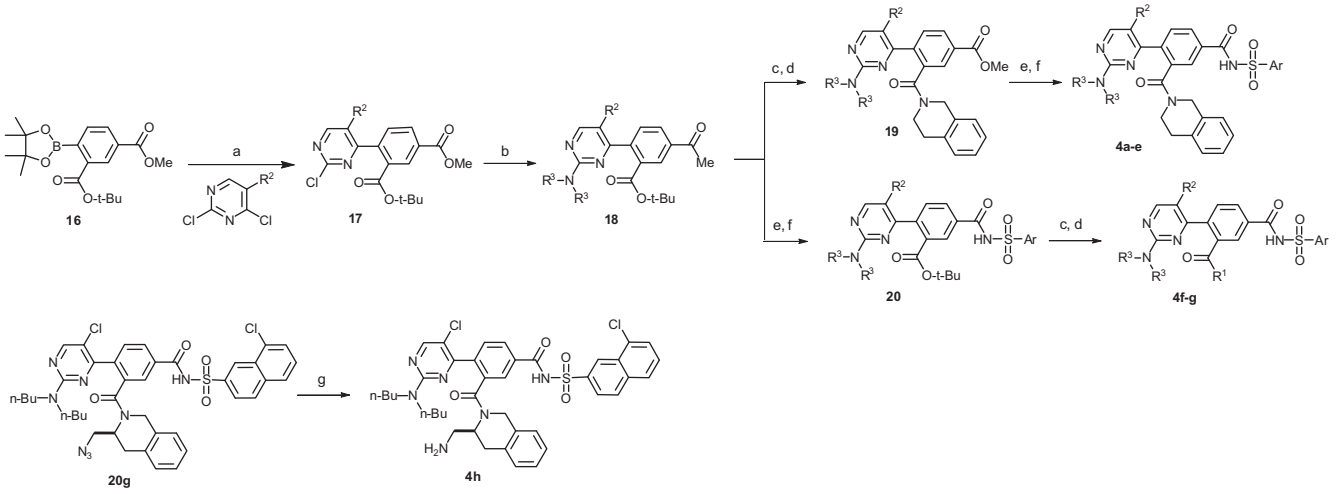

Scheme 2. Reagents and conditions: (a) $PdCl_2dppf_2$, Na_2CO_3, 1,4-dioxane, 80 °C, 15 h, 78%; (b) $NH(R^3)_2$, K_2CO_3, DMF, 60 °C, 5–12 h, >80%; (c) TFA/DCM, 100%; (d) THIQ, HATU, DIPEA, rt, 2 h, 52–80%; (e) 2 N aqueous NaOH, THF/MeOH, rt, 2–3 h, 90–100%; (f) sulfonamide **15**, EDC, DMAP, rt, 57–70%, (g) Pd/C, H_2, MeOH, rt, 2 h, 57%.

inhibitor of Bcl-2 and Bcl-xL. Introduction of amine substituted THIQ **3q** was also well tolerated giving IC_{50}'s against Bcl-2 and Bcl-xL of 24 and 7 nM, respectively.

Lastly, SAR of the acylsulfonamide was explored (Table 2). Replacement of the aromatic naphthyl ring with a trimethylsilylethyl group (**3r**) was found to be detrimental for Bcl-2 activity (3-fold less active than **3d**), but inconsequential with regards to Bcl-xL activity. The simple ethyl acylsulfonamide (**3s**) was determined to be less potent for both enzymes. Extending the alkyl group from ethyl to pentyl as in compound **3t** restored some Bcl-2 activity (IC_{50} = 65 nM) but had no effect on Bcl-xL (IC_{50} = 120 nM). Substitution of the naphthyl ring with a chloride in the 8-position (**3u**) gave a slight improvement in both Bcl-2 and Bcl-xL activity as compared to unsubstituted naphthyl **3j**.

An X-ray crystal structure of compound **3r** complexed to Bcl-xL demonstrated that these pyrazole-based inhibitors bind in the conserved hydrophobic groove normally occupied by pro-apoptotic family members such as Bim (Fig. 2).[13] As designed, the THIQ moi-

Table 1
Regioisomeric pyrazoles: pyrazole ring SAR[a]

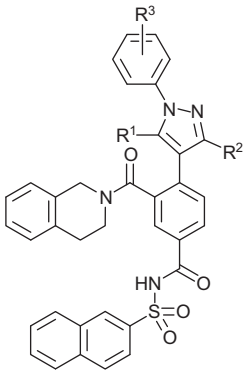

Compd	R^1	R^2	R^3	IC_{50} (μM)	
				Bcl-2	Bcl-xL
3a	Me	CO_2Et	H	4.19	0.64
3b	Bu	CO_2Et	H	0.66	0.042
3c	Bu	CO_2H	H	0.17	0.030
3d	Bu	CH_2OH	H	0.061	0.011
3e	Bu	CO_2Et	4-OMe	1.79	0.048
3f	Bu	CO_2Et	3-OPh	0.14	0.47
3g	Bu	CO_2Et	4-OPh	0.10	0.055
3h	Bu	CH_2OH	4-OPh	0.13	0.035
3i	Bu	CH_2OH	4-O(Ph, 4-Cl)	0.022	0.035
3j	Bu	CH_2OH	4-O(Ph, 3-Cl)	0.008	0.018
3k	Bu	CH_2OH	4-OButyl	0.045	0.026
3l	Bu	CH_2OH	4-Ph	0.007	0.013
3m	Bu	CH_2OH	4-$(CH_2)_2OH$	0.020	0.006
3n	Bu	CH_2OH	4-$(CH_2)_3OH$	0.014	0.007
3o	Bu	CH_2OH	3-CH_2OH	0.071	0.015

[a] For assay conditions see Ref. 9.

Table 2
Regioisomeric pyrazoles: THIQ and acylsulfonamide SAR[a]

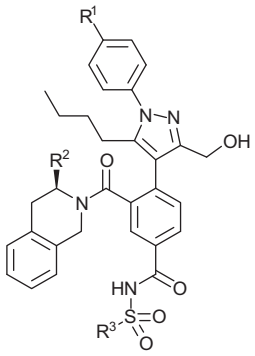

Compd	R^1	R^2	R^3	IC_{50} (μM)	
				Bcl-2	Bcl-xL
3d	H	H	Naphthyl	0.061	0.011
3p	H	CH_2OH	Naphthyl	0.011	0.008
3q	H	CH_2NH_2	Naphthyl	0.024	0.007
3r	H	H	$(CH_2)_2TMS$	0.19	0.013
3s	O(3-Cl)Ph	H	CH_2CH_3	0.19	0.14
3t	O(3-Cl)Ph	H	$(CH_2)_4CH_3$	0.065	0.12
3u	O(3-Cl)Ph	H	Naphthyl, 8-Cl	0.006	0.015

[a] For assay conditions see Ref. 9.

ety resides in the I95 pocket and interacts with Phe97, Tyr101, and Phe105 via a combination of π-stacking and edge-face interactions. The pyrazole C-5 butyl group extends into the L92 pocket. The loss in potency in shortening this butyl group to a methyl as in **3a** can now be rationalized as the methyl group is not long enough to fill this hydrophobic space normally occupied by the amino acid side chain of leucine. The pyrazole *N*-1 phenyl ring points to the I88 pocket and biaryls such as **3j** likely extend into this space. The alcohol at C-3 of the pyrazole ring makes a hydrogen bond with Leu130. Finally, the acyl sulfonamide forms several critical interactions with the Bcl-xL protein. For example, the acyl sulfonamide carbonyl accepts a hydrogen bond from the Tyr101 hydroxyl group. The trimethylsilylethyl group projects into a rather large hydrophobic pocket defined by Ala93, Phe97, Arg100, Val141, and Tyr195. Normally occupied by Phe99 of Bim, it is clear that groups like naphthyl would be well accomodated in such an environment.

Next, we applied lessons learned from the pyrazole series to the design of 2-aminopyrimidine based antagonists (Table 3). The parent compound in this series, pyrimidine **4a**, gave modest potency against Bcl-2 (IC_{50} = 700 nM) and Bcl-xL (IC_{50} = 500 nM). Addition of a halide (**4b**,**c**) to the naphthyl ring gave approximately five-fold improvement in Bcl-2 activity, but had little effect on Bcl-xL. Likewise, replacement of the naphthyl ring by 1-(3,4-dichlorobenzyl)indoline to give **4d** had a similar effect. As before, addition of amino- or hydroxy- methyl groups at the THIQ 3-position gave improved results (**4e**,**f**). A significant discovery came from the observation that substitution of the pyrimidine ring at C-5 with

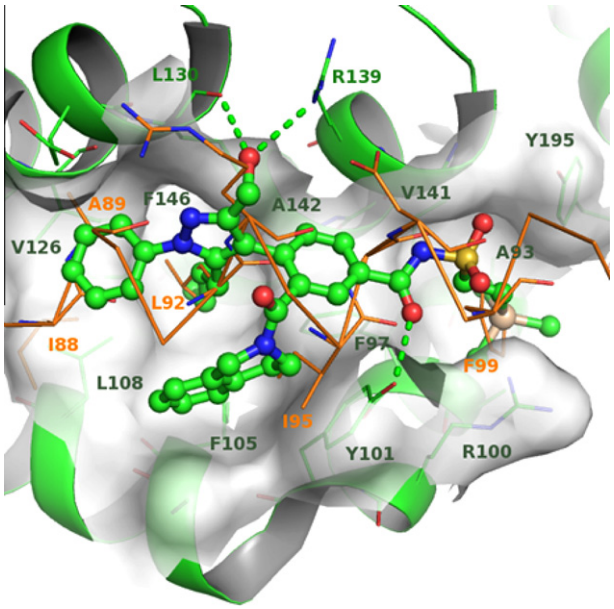

Figure 2. Co-crystal structure of compound **3r** in Bcl-xL (green) superimposed with Bim from the Bim/Bcl-xL complex 1PQ1 (orange). The Bim residues mimicked by **3r** (I88, A89, L92, I95, and F99) are labeled in orange. Key interactions between **3r** and Bcl-xL are labeled in green. The hydrogen bonds to the side chain hydroxyl from Y101 and the backbone carbonyl of L130 are denoted with dashed lines.

chloro or methyl groups led to improvement in potency (**4g**,**h**). Finally, replacement of the dibutylamino group on the pyrimidine ring with dipropylamino (**4i**) was optimum as the ethyl and pentyl analogs showed diminished activity (data not shown). Compounds from this series are expected to bind Bcl-2 and Bcl-xL analogously to pyrazole **3r**. Molecular modeling suggests the dipropylamine

Table 3
2-Aminopyrimidines[a]

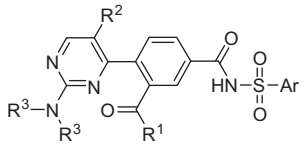

Compd	Ar	R^1	R^2	R^3	IC_{50} (μM)	
					Bcl-2	Bcl-xL
4a	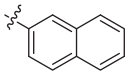	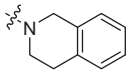	H	*n*-Butyl	0.70	0.50
4b	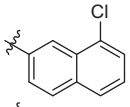	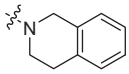	H	*n*-Butyl	0.12	0.48
4c	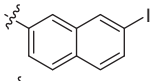	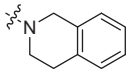	H	*n*-Butyl	0.14	0.97
4d	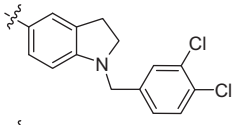	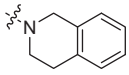	H	*n*-Butyl	0.12	0.71
4e	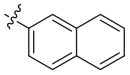	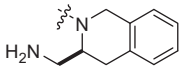	H	*n*-Butyl	0.43	0.16
4f	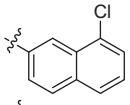	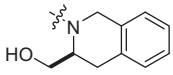	H	*n*-Butyl	0.16	0.13
4g	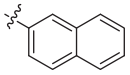	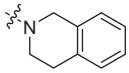	Cl	*n*-Butyl	0.16	0.23
4h	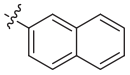	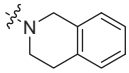	CH_3	*n*-Butyl	0.11	0.12
4i	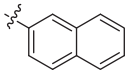	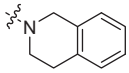	H	*n*-Propyl	0.15	0.25
4j	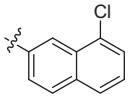	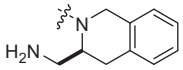	Cl	*n*-Propyl	0.015	0.014
4k	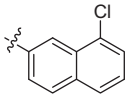	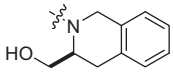	Cl	*n*-Propyl	0.009	0.009

[a] For assay conditions see Ref. 9.

simultaneously fills both the I88 and L92 pockets which explains why the length of the alkyl chain is so critical.

Optimized acylsulfonamide, THIQ, and pyrimidine substituents were combined to give pyrimidines **4j** and **4k**. These compounds demonstrated potent dual Bcl-2/Bcl-xL activity with greater than 50-fold improvement in activity compared to the parent compound **4a**.

Several compounds from the regioisomeric pyrazole and 2-aminopyrimidine series were examined for their effects on cell proliferation in Bcl-2/Bcl-xL dependent cell lines (Table 4).[14] Cellular antiproliferative activity paralleled that observed in the biochemical assays with potent dual antagonists from the pyrazole series (**3j**, **3u**) performing better than less potent analogs (**3k**, **3o**). The most potent compounds in the cell proliferation assay came from the aminopyrimidine series with compounds **4j** and **4k** demonstrating submicromolar activity in the MV-4-11 AML cell line. In addition, pyrimidine **4j** maintained submicromolar activity in MV-4-11 cells in the presence of 10% fetal calf serum (IC_{50} = 0.73 μM).

With compounds in hand demonstrating excellent biochemical potency against Bcl-2 and Bcl-xL, select analogs were examined in isolated mitochondria from MV-4-11 AML cells for cytochrome c release and BAK oligomerization (Fig. 3).[15] Pyrimidines **4j** and **4k** were tested at concentrations of 0.1 and 1 μM and were shown to induce cytochrome c release and BAK oligomerization in a dose-dependent manner. These results demonstrate **4j** and **4k** antagonize Bcl-2 and Bcl-xL function on the surface of mitochondria, resulting in initiation of the intrinsic apoptotic pathway. Pyrazoles such as **3j** and **3o** also demonstrated cytochrome c release and BAK oligomerization at low concentrations, however, they

Table 4
Cellular antiproliferative activity (2% FCS)[a]

Compd	SUDHL-4 IC_{50} (μM)	MV-4-11 IC_{50} (μM)
3j	2.35	0.70
3k	2.49	1.43
3o	>10	5.06
3u	2.02	0.58
4j	6.64	0.33
4k	3.79	0.33

[a] For assay conditions see Ref. 9.

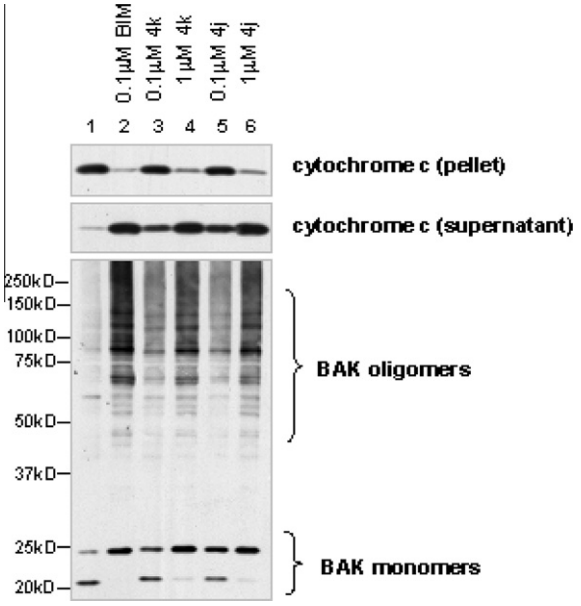

Figure 3. Cytochrome c release and BAK oligomerization from isolated mitochondria of MV-4-11 cells.

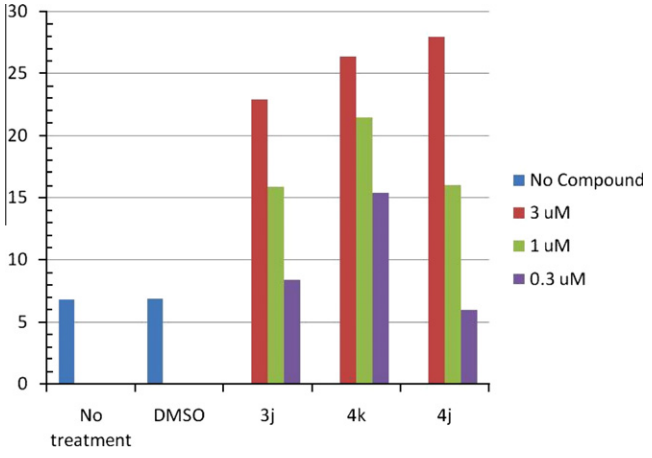

Figure 4. Average percent population of depolarized mitochondria in MV-4-11 cells.

failed to show induction of BAK oligomerization at higher concentrations (data not shown). This may be due to poor aqueous solubility at higher concentrations.

Finally, pyrazole **3j** and pyrimidines **4j** and **4k** were tested for their effects on mitochondria depolarization in whole cells (Fig. 4).[16] All three compounds induced ~25% depolarized mitochondria in MV-4-11 AML cells after treatment for 7 h at a concentration of 3 μM.[17] This activity provides further mechanistic evidence of Bcl-2 and Bcl-xL inhibition.

In summary, potent pyrazole and pyrimidine acylsulfonamide inhibitors with dual activity against Bcl-2 and Bcl-xL were identified. Compounds were optimized for binding to essential pockets such as I88, L92, I95, and F99 which are normally occupied by pro-apoptotic family members. An X-ray co-crystal structure with Bcl-xL confirmed the proposed binding mode. Compounds demonstrated on-target mechanistic inhibition of Bcl-2 and Bcl-xL through cytochrome c release and BAK oligomerization in isolated mitochondria. Further evidence of target inhibition was demonstrated by whole cell mitochondria depolarization in MV-4-11 cells. Improved cellular antiproliferative activity was achieved relative to the original lead pyrazole typified by **2**.

References and notes

1. For recent reviews see: (a) Chipuk, J. E.; Green, D. R. *Trends Cell Bio.* **2008**, *18*, 157; (b) Youle, R. J.; Strasser, A. *Nature Rev. Mol. Cell Biol.* **2008**, *9*, 47; (c) Leber, B.; Lin, J.; Andrews, D. W. *Oncogene* **2010**, *29*, 5221; (d) Tait, S. W. G.; Green, D. R. *Nature Rev. Mol. Cell Bio.* **2010**, *11*, 1.
2. Sperandio, O.; Reynes, C. H.; Camproux, A.-C.; Villoutreix, B. O. *Drug Discov. Today* **2010**, *15*, 220. and references therein.
3. Cummings, C. G.; Hamilton, A. D. *Curr. Opin. Chem. Biol.* **2010**, *14*, 1.
4. Vogler, M.; Dinsdale, M.; Dyer, M. J. S.; Cohen, G. M. *Cell Death Differ.* **2009**, *16*, 360.
5. Barelier, S.; Pons, J.; Marcillat, O.; Lancelin, J.-M.; Krimm, I. *J. Med. Chem.* **2010**, *53*, 2577.
6. (a) Bruncko, M.; Oost, T. K.; Belli, B. A.; Ding, H.; Joseph, M. K.; Kunzer, A.; Matineau, D.; McClellan, W. J.; Mitten, M.; Ng, S.-C.; Nimmer, P. M.; Oltersdorf, T.; Park, C.-M.; Petros, A. M.; Shoemaker, A. R.; Song, X.; Wang, X.; Wendt, M. D.; Zhang, H.; Fesik, S. W.; Rosenberg, S. H.; Elmore, S. W. *J. Med. Chem.* **2007**, *50*, 641; (b) Park, C.-M.; Bruncko, M.; Adickes, J.; Bauch, J.; Ding, H.; Kunzer, A.; Marsh, K. C.; Nimmer, P.; Shoemaker, A. R.; Song, X.; Tahir, S. K.; Tse, C.; Wang, X.; Wendt, M. D.; Yang, X.; Zhang, H.; Fesik, S. W.; Rosenberg, S. H.; Elmore, S. W. *J. Med. Chem.* **2008**, *51*, 6902.
7. (a) Tse, C.; Shoemaker, A. R.; Adickes, J.; Anderson, M. G.; Chen, J.; Jin, S.; Johnson, E. F.; Marsh, K. C.; Mitten, M. J.; Nimmer, P.; Roberts, L.; Tahir, S. K.; Xiao, Y.; Yang, X.; Zhang, H.; Fesik, S.; Rosenberg, S. H.; Elmore, S. W. *Cancer Res.* **2008**, *68*, 3421; (b) Ackler, S.; Mitten, M. J.; Foster, K.; Oleksijew, A.; Refici, M.; Tahir, S. K.; Xiao, Y.; Tse, C.; Frost, D. J.; Fesik, S. W.; Rosenberg, S. H.; Elmore, S. W.; Shoemaker, A. R. *Cancer Chemother. Phamacol.* **2010**, *66*, 869.
8. Vogler, M.; Furdas, S. D.; Jung, M.; Kuwana, T.; Dyer, M. J. S.; Cohen, G. M. *Clin. Cancer Res.* **2010**, *16*, 4217.
9. Perez, H. L.; Banfi, P.; Bertrand, J.; Cai, Z.-W.; Grebinski, J.; Kim, K.; Lippy, J.; Modugno, M.; Naglich, J.; Schmidt, R. J.; Tebben, A.; Vianello, P.; Wei, D. D.; Zhang, L.; Galvani, A.; Lombardo, L. J.; Borzilleri, R. M. *Bioorg. Med. Chem. Lett.* **2012**, *22*. preceding paper.
10. Mei, T.-S.; Giri, R.; Maugel, N.; Yu, J.-Q. *Angew. Chem., Int. Ed.* **2008**, *47*, 5215.
11. Deng, X.; Mani, N. S. *Org. Lett.* **2008**, *10*, 1307.
12. Miura, M.; Koike, T.; Ishihara, T.; Hirayama, F.; Sakamoto, S.; Okada, M.; Ohta, M.; Tsukamoto, S.-I. *Synth. Commun.* **2006**, *36*, 3809.
13. The structure was deposited in the PDB as 4EHR.
14. Deng, J.; Carlson, N.; Takeyama, K.; Dal Cin, P.; Shipp, M.; Letai, A. *Cancer Cell* **2007**, *12*, 171.
15. For assay conditions see Ref. 9.
16. Representative characterization data: (a) **3j**; ^{1}H NMR (CD_3OD) δ 8.73 (s, 1H), 8.12–7.98 (m, 6H), 7.73–7.66 (m, 2H), 7.63–6.94 (m, 13H), 4.62–4.18 (m, 4H), 3.65–3.17 (m, 2H), 2.79–2.45 (m, 4H), 1.31–0.91 (m, 4H), 0.65–0.58 (m, 3H); MS(ESI$^+$) *m*/*z* 825.1 $(M+H)^+$; (b) **4j**, ^{1}H NMR ($CDCl_3$, 1:1 mixture of amide rotamers) δ 9 .16 (s, 1H), 8.42–8.14 (m, 4 H), 8.02 (d, *J* = 8.1 Hz, 1H), 7.82 (d, *J* = 8.6 Hz, 1H), 7.76–7.47 (m, 5H), 7.15–7.04 (m, 2 H), 6.94 (d, *J* = 6.0 Hz, 0.5H), 6.85 (d, *J* = 6.0 Hz, 0.5H), 5.43 (br s, 1H), 4.48 (d, *J* = 17.6 Hz, 1H), 4.28 (d, *J* = 17.6 Hz, 1H), 3.45–2.98 (m, 5H), 2.88–2.48 (m, 5H), 1.65–1.23 (m, 4H), 1.01–0.51 (m, 6H); MS(ESI$^+$) *m*/*z* 745.1 $(M+H)^+$; (c) **4k**, ^{1}H NMR (CD_3OD, 1:1 mixture of amide rotamers) δ 9.05 (s, 1H), 8.96 (br s, 1H), 8.24 (br s, 1H), 8.14–8.04 (m, 2H), 7.85–7.49 (m, 5H), 7.16–6.89 (m, 3H), 6.82 (br s, 1H), 5.22–5.05 (m, 1H), 4.53 (br s, 1H), 4.24 (br s, 1H), 3.45–3.05 (m, 5H), 2.80–2.34 (m, 3H), 1.65–1.50 (m, 4H), 0.99–0.52 (m, 6H); MS(ESI$^+$) *m*/*z* 746.1 $(M+H)^+$.
17. Whole cell depolarization assay: The human acute myeloid leukemia (AML) cell line, MV-4-11 (CRL-9591), was purchased from the American Type Culture Collection (Manassas, VA) and routinely maintained in RPMI 1640 medium (GIBCO, Carlsbad, CA) supplemented with 10% fetal bovine serum at 37 °C in humidified atmosphere of 5% CO_2. Logarithmically growing cells were concentrated by low-speed centrifugation, suspended in serum-free RPMI-1640 medium and stained using the cationic dye, MitoProbe JC-1 (2 μM, 0.5% DMSO, 30 min, 37 °C), following the manufacturer's instructions (Molecular Probes, Eugene, OR). Stained cells were concentrated by low-speed centrifugation, suspended in RPMI-1640 medium supplemented with 2% fetal bovine serum and subjected to compound treatment (5×10^5 per well of a 96-well plate, 7 h, 37 °C). Cellular mitochondria depolarization was measured by flow cytometry (FACSCanto II, BD Biosciences, San Jose, CA) and the data analyzed using FlowJo software (Tree Star Inc., Ashland, OR).